Recursive Clifford noise reduction

Aharon Brodutch,¹ Gregory Baimetov,^{1,2} Edwin Tham,¹ and Nicolas Delfosse¹

¹IonQ Inc.

²Department of Mathematics, University of Washington, Seattle, WA 98195-4350

(Dated: November 2025)

Clifford noise reduction CliNR is a partial error correction scheme that reduces the logical error rate of Clifford circuits at the cost of a modest qubit and gate overhead. The CliNR implementation of an n-qubit Clifford circuit of size s achieves a vanishing logical error rate if $snp^2 \to 0$ where p is the physical error rate. Here, we propose a recursive version of CliNR that can reduce errors on larger circuits with a relatively small gate overhead. When $np \to 0$, the logical error rate can be vanishingly small. This implementation requires $(2 \lceil \log(sp) \rceil + 3) n + 1$ qubits and at most $24s \lceil (sp)^4 \rceil$ gates. Using numerical simulations, we show that the recursive method can offer an advantage in a realistic near-term parameter regime. When circuit sizes are large enough, recursive CliNR can reach a lower logical error rate than the original CliNR with the same gate overhead. The results offer promise for reducing logical errors in large Clifford circuits with relatively small overheads.

I. INTRODUCTION

Two major obstacles for reaching utility scale quantum computation are increasing the number of qubits and reducing error rates. Quantum error correction (QEC) offers a way to reduce the logical error rates at the cost of increasing physical resources in a scalable way [1, 2]. Current quantum computers do not support enough qubits for full-fledged fault-tolerant QEC. Moreover, the overheads for implementing fault-tolerant logical operations are high, both in qubit and gate counts, notwithstanding huge improvements over the last few years [3–6]. At the same time, physical error rates and raw qubit counts are already sufficient for showing the advantage of quantum computers [7–9]. These results provide some evidence that fault-tolerant QEC might not be necessary to show some initial utility scale computation, especially if methods for error mitigation and partial error correction can be used to reduce the impact of errors [10].

Error-mitigation (EM) refers to a collection of techniques aimed at reducing the impact of errors on the output of a quantum computer. Typically, EM techniques re-shape noise (e.g. twirling [11]), post-select shots identified as erroneous (e.g. flag error-detection [12, 13]), post-process noisy data (e.g. filtering [14]), or a combination thereof [15]. Of particular interest are coherent Pauli checks (CPC) [12, 13, 16] that require no explicit encoding, and are readily applied to application circuits with few ancilla gubit overheads. The main disadvantages of CPC are that it is limited to reducing errors in Clifford circuits and that any single detected error requires the shot to be discarded and the computation restarted anew. As a result of the latter, the restart rate approaches unity, as circuit size grows. Clifford Noise Reduction CliNR [17] deals with this problem by building Clifford subcircuits offline and injecting them into the main circuit when they pass verification. The result is a low-overhead scheme that can be used to reduce logical error rates in Clifford subcircuits. The method is however limited to subcircuits of size at most of the order of $1/(np^2)$ where p is the physical error rate and n is the number of qubits. Here we present a generalization of CliNR which we call Recursive CliNR. It provides low-overhead error reduction for sub-circuits of any size s, as long as np is sufficiently small. As in [17], we provide an analytical proof that this is asymptotically true for a simple noise model with no idle noise and provide numerical evidence for more complex noise models.

Recursive CliNR, recursively applies CliNR to a sequence of CliNR sub-circuits. The main advantage is that the injection circuits, which don't get verified in the standard CliNR, will now get verified at the next level of the recursion. However, new unverified injection steps are introduced at the next level. These get verified at the next level etc., with the aim of ultimately having a small number of unverified injection steps at the top level. The number of CliNR subcircuits (each with its injection step) at each level of the recursion is determined by a tree which we call the CliNR tree. The right choice of parameters for this tree can lead to better performance than standard CliNR - lower logical error rates at the same circuit size.

The rest of this paper is organized as follows. In the next section we review some background material including the noise model and the original CliNR scheme. We identify the main source of errors that cannot be detected and the limitation of the scheme. In Section III we introduce Recursive CliNR and the CliNR tree used in its construction. An algorithm for constructing the corresponding circuit is provided in Algorithm 1. In Section IV we introduce a specific implementation of Recursive CliNR called the *uniformly bounded* implementation. It allows us to make our main statement (Theorem 1): Recursive CliNR can be used to reach a vanishing logical error rate with a gate overhead that's polynomial in sp, as long as $np \to 0$. We do this using a sequence of technical statements which we prove in Section IV C. In Section V we present numerical results that show the advantage of Recursive CliNR at n = 70 and n = 400. In the conclusion section (Section VI) we discuss potential improvements to the implementation.

II. BACKGROUND

In this section, we review the standard circuit-level noise model and the original CliNR scheme [17].

A. Noise model

We consider quantum circuits containing single-qubit preparations, unitary gates and single-qubit measurements. An important class of quantum circuits is the set of n-qubit Clifford circuits. These circuits act on n-qubit input states in the same way as a Clifford unitary U (potentially after discarding ancillas). A Clifford unitary preserves Pauli operators by conjugation, i.e. for all Pauli operators P, the operation UPU^{\dagger} is also a Pauli operator.

We consider the standard circuit-level noise model where each circuit operation is followed by a random Pauli error with rate p. The Pauli error is selected uniformly in the set of non-trivial Pauli errors acting on the support of the operation. Measurement noise is represented by a flip of the measurement outcome with probability p. Errors corresponding to different operations are assumed to be independent. In our simulation we also include idle noise and use different error rates for different options (see Section V).

The circuit-level noise model introduces errors in a quantum circuit, which translate into errors on the output state of the circuit, that we call the *output error*.

An implementation of a Clifford circuit C is a circuit C' that produces the same output state as C for any input state in the absence of error. The circuit-level noise induces a probability distribution over the set of output errors of an implementation. The logical error rate of an implementation is defined to be the probability that the output error has a non-trivial effect on the output of the circuit. We say that an implementation is ideal when the logical error rate is 0, otherwise we say that the implementation is noisy.

The most naive implementation of a circuit is its direct implementation C'=C. In general, an implementation C' of a Clifford circuit C uses additional qubits and gates. The extra qubits are traced out before the end of the circuit. The qubit overhead, $\omega_{\rm Q}$, is defined as the number of qubits of C' divided by the number of qubits in C. The gate overhead, $\omega_{\rm G}$, is the expected number of gates in C' divided by the number of gates in C' divided by the number of gates in C. A gate may be executed multiple times because of a repeat until success loop for instance. Then, it is counted as many times as it is repeated in the gate overhead.

Throughout this work we divide the implementation of a Clifford circuit C into blocks. If a fault during block B has a non-trivial effect on the output of B then we say that it is a $logical\ error\ in\ B$. A logical error in B does not necessarily imply a logical error in the implementation of C.

B. Review of CliNR

CliNR was introduced in [17] as a protocol that can reduce the logical error rate in the implementation of a Clifford circuit. Consider a unitary n-qubit Clifford circuit C, called the *input circuit*, with size s (*i.e.* C has s unitary gates). Given an integer r, the CliNR implementation, denoted CliNR_{1,r}(C), is defined as the following 3 step process (see Fig. 1):

- 1. Resource state preparation (RSP). A 2n-qubit resource (stabilizer) state $|\varphi\rangle$ is prepared as follows. First n Bell pairs are prepared (using at most $A_P n$ noisy gates). Next, the circuit C is implemented on n of these qubits, one from each pair. The implementation of C requires s noisy gates.
 - The resource state $|\varphi\rangle$ generated by an ideal implementation of RSP is stabilized by a stabilizer group $S(\varphi)$. An error during the noisy implementation of RSP produces a state $E|\varphi\rangle$. If E does not commute with $S(\varphi)$ then it is a logical error in RSP.
- 2. Resource state verification (RSV). The resource state is verified by measuring r stabilizers using stabilizer measurements. Here we assume that the stabilizers are chosen randomly and uniformly from $S(\varphi)$, but other choices can lead to better performance [18]. A logical error in RSP has probability 1/2 to commute with a stabilizer chosen at random from $S(\varphi)$. In an ideal implementation of the stabilizer measurement, a logical error that anti-commutes with the stabilizer is detected. If an error is detected we restart from RSP. In a noisy implementation an error during the stabilizer measurement can lead to a false detection or to a subsequent logical error. Each stabilizer measurement requires a single ancilla. We can define constants A_V and B_V such that the implementation of RSV requires at most $A_V n + B_V$ noisy gates. An ideal implementation will reduce the logical error rate by a factor of 2^r (see Lemma 1).
- 3. Resource state injection (RSI). If no errors are detected during RSV, the subcircuit C is applied to an n-qubit input state by consuming the resource state $|\varphi\rangle$. We can define a constant A_I such that this process takes at most A_In noisy gates. The rails hosting the input state (top 3 rails in Fig. 1 (a) and (b)) are called the *input rails*.

Therein and throughout this work, A_P , A_V , B_V and A_I are constants as defined above. These depend on the specifics of the implementation, but are independent of s, p, n and C. We refer to these three parts as the RSP, RSV and RSI blocks e.g. RSI block refers to the implementation of the RSI circuit in Fig. 1 (b). A CliNR₁ block refers to the implementation of the entire circuit in Fig. 1 (b). We use CliNR₁ as a general term for the CliNR protocol above, to distinguish it from Recursive CliNR defined in Section III.

When C is long, it can be advantageous to break it down into t subcircuits C_i and then apply $\operatorname{CliNR}_{1,r}$ to each subcircuit. The logical error rate and restart rate in each $\operatorname{CliNR}_{1,r}(C_i)$ block are lower than in $\operatorname{CliNR}_{1,r}(C)$ leading to an advantage for t>1 in some parameter regimes. In [17] this technique (called CliNR_t) was used to show that it is possible to achieve a vanishing logical error rate when $\operatorname{snp}^2 \to 0$. The gate overhead in this regime can be bounded by $\omega_{\mathbf{G}} \leq 2$.

One disadvantage of this technique is that errors during each RSI block cannot be detected. In the following, we tackle this issue with a recursive CliNR scheme. This scheme exploits the fact that $CliNR_1$ blocks are Clifford circuits which can themselves be used as the input circuit for a larger $CliNR_1$ block.

III. RECURSIVE CLINR

This section introduces the recursive generalization of CliNR which we call Recursive CliNR. We begin with the CliNR tree.

An ordered tree is a rooted tree such that for any vertex u, the children of u have a specific order v_0, v_1 , etc. If a tree is ordered, we can label its vertices as $v_{\ell,i}$, where $\ell \in \mathbb{N}$ is the distance to the root, which we call the level, and i is the index of the vertex among the vertices at level ℓ . For example, the vertices of a 4-regular tree are indexed as $v_{0,0}, v_{1,0}, v_{1,1}, v_{1,2}, v_{1,3}, v_{2,0}, v_{2,1},$ etc. Fig. 2 (a) shows an example of ordered tree with labeled vertices.

A CliNR tree, denoted $\mathcal{T}(\mathbf{s}, \mathbf{r})$ or simply \mathcal{T} , is a finite ordered tree, equipped with two functions \mathbf{s} and \mathbf{r} defined over the vertex set of \mathcal{T} . These functions assign nonnegative integers $\mathbf{s}(u)$ and $\mathbf{r}(u)$ to each vertex u of the tree. We require that, for any vertex u, the sum of the values $\mathbf{s}(v)$ associated with its children v is equal to $\mathbf{s}(u)$.

Let \mathcal{T} be a CliNR tree with depth D and let C be a n-qubit Clifford circuit with size $\mathbf{s}(v_{0,0})$. For all levels $\ell = 0, 1, \ldots, D$, we have $\sum_i \mathbf{s}(v_{\ell,i}) = \mathbf{s}(v_{0,0})$ where i runs over the indices of all the vertices at level ℓ of the tree. It is possible to write C as the concatenation of subcircuit. $C_{\ell,0}, C_{\ell,1}, \ldots$ where $C_{\ell,i}$ is a subcircuit of C with size $\mathbf{s}(v_{\ell,i})$. Moreover, for all $\ell \leq D-1$, the circuit $C_{\ell,i}$ is the concatenation of the subcircuits $C_{\ell+1,j}$ where $v_{\ell+1,j}$ runs over the children of $v_{\ell,i}$ in \mathcal{T} .

The recursive CliNR implementation of C, denoted CliNR(\mathcal{T}, C), is the implementation obtained by applying the procedure described in Algorithm 1 to the circuit C. Fig. 2 (c) provides the circuit for the implementation of CliNR(\mathcal{T}, C) where \mathcal{T} is the tree in Fig. 2 (a).

In Algorithm 1, we do not use the value of \mathbf{r} at the root. One could extend the construction by adding $\mathbf{r}(v_{0,0})$ stabilizer measurements at the end of the circuit.

The implementation $\operatorname{CliNR}(\mathcal{T}, C)$ is a proper generalization of the CliNR implementations introduced in [17]. Indeed, we recover the implementation $\operatorname{CliNR}_{1,r}(C)$ by taking a tree with two vertices $v_{0,0}$ and $v_{1,0}$ such that $\mathbf{r}(v_{1,0}) = r$. The implementation $\operatorname{CliNR}_{t,r}(C)$ is derived

```
Algorithm 1: Algorithm for constructing a recursive CliNR circuit
```

input: A n-qubit Clifford circuit C and a CliNR tree

```
\mathcal{T} = \mathcal{T}(\mathbf{s}, \mathbf{r}).
output: The implementation \mathrm{CliNR}(\mathcal{T}, C) of C.

1 Set C' = C_{0,0}.

2 Add one ancilla to C'.

3 for all level \ell = 0, 1, \dots, D-1 do

4 Add 2n ancilla qubits to C'.

5 for all vertices v_{\ell+1,j} do

6 Let r = \mathbf{r}(v_{\ell+1,j}).

7 Replace the sub-circuit C_{\ell+1,j} inside C' by \mathrm{CliNR}_{1,r}(C_{\ell+1,j}) using the 2n+1 ancilla qubits added at level \ell.

8 return C'.
```

from a depth-one tree with a root and t children $v_{1,j}$ for $j = 0, 1, \ldots, t-1$ with $\mathbf{r}(v_{1,j}) = r$.

There are many possible choices for the stabilizers used to define $CliNR(\mathcal{T}, C)$. The only requirement is that they belong to the stabilizer group of the resource state consumed by in $CliNR_{1,r}$ in Algorithm 1. Here, we select random stabilizer generators following [17]. Optimization strategies to select these stabilizers more carefully were proposed recently in [18].

The following is a direct consequence of Algorithm 1:

Proposition 1 (qubit overhead for Recursive CliNR). The recursive implementation of an n-qubit Clifford circuit requires (2D+1)n+1 qubits.

When $n \to +\infty$ the qubit overhead is $\omega_Q \to 2D+1$. For D=1, we recover the $3\times$ qubit overhead of the original CliNR scheme as expected. In the conclusions (Section VI) we briefly discuss other implementations that may perform better at the cost of larger qubit overheads. Gate overheads and logical error rates are studied and discussed in what follows.

IV. THE UNIFORMLY BOUNDED CLINR IMPLEMENTATION

Our main result below shows that when $np \to 0$ it is possible to implement Recursive CliNR with a vanishing logical error rate. To assist with the proof, we define the Uniformly bounded implementation (for a formal definition see Definition 1). This implementation ensures that every iterative use of $\text{CliNR}_{1,r}$ has an input circuit with a logical error rate bounded by 2/3 and an output state with a logical error rate upper bounded by a function of order np (see Fig. 2 (b)). The logical error rate for the full implementation is therefore bounded by a function of order t_1np where t_1 is the number of vertices at level 1. For sufficiently large D, we get $t_1 = 1$. In this case the logical error rate is bounded from above and below by functions of order np.

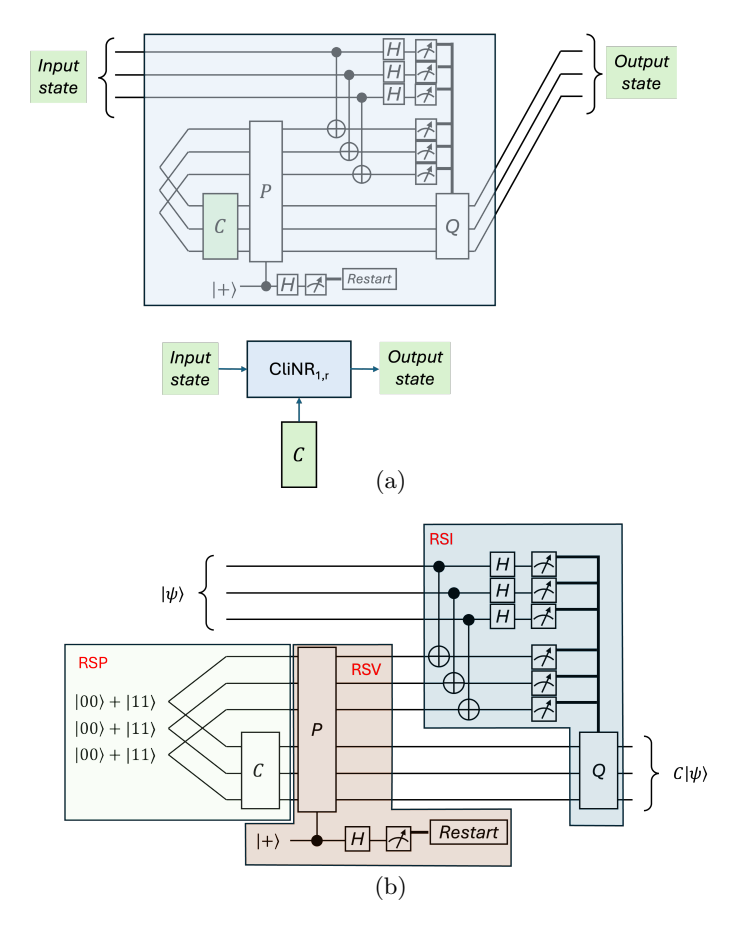


FIG. 1. A CliNR₁ circuit. (a) Schematic of the main components for a CliNR circuit, input state, output state, and input circuit C. (b) The 3 blocks used to build a CliNR circuit: resource state preparation (RSP), resource state verification (RSV) and resource state injection (RSI). The number of noisy gates in each of these blocks is $A_P n + s$, $(A_V n + B_V)r$ and $A_I n$ respectively. A_P, A_V, B_V, A_I are constants that depend on the implementation (e.g. number of noisy gates used to implement a stabilizer measurement). For simplicity only a single stabilizer measurement is shown in RSV, in general the RSV block will have multiple stabilizer measurements, all of these can use the same ancilla (bottom rail).

A schematic of the implementation is given in Fig. 2. At the bottom level $(\ell=D)$ we choose subcircuit $C_{D,j}$ with size at most $\bar{s}_D = \left\lfloor \frac{2}{3p} \right\rfloor$. We then choose $r_{D,j}$ to bound the logical error rate from RSP to the same order as the logical error rate from RSV. This can be done by fixing all $r_{\ell,j} = R$ (defined in Eq. (10)). The logical error rate for CliNR₁ is then bounded by Anp where A is a constant (see proof of Lemma 5). At the next level up (and iteratively up to level 1) we take groups of T vertices such that $TAnp \leq 2/3$ and feed them to the next vertex up ensuring that the logical error rate of each individual CliNR₁ implementation in Algorithm 1 is bounded by Anp.

A. Main result

Here, we state the main result of this paper which proves that the recursive CliNR scheme introduced in this work can achieve a vanishing logical error rate for n-qubit Clifford circuits with arbitrary size as long as $np \to 0$. For comparison, the standard CliNR scheme is limited to circuits size $s = o(1/(np^2))$.

Theorem 1. Consider the family of n-qubit Clifford circuits C of size s with physical error rate p and let $D = \max\{1, \lceil \log(sp) + 1 \rceil\}$. If $np \to 0$ there is a recursive CliNR implementation with a vanishing logical error rate, a gate overhead $\omega_G \leq 24 \lceil (sp)^4 \rceil$, and a qubit overhead of $\omega_Q = (2D+1)+1/n$.

Here and throughout this paper, log denotes the base 2 logarithm and $\omega_{\rm G}$, $\omega_{\rm Q}$ are the CliNR gate and qubit overheads respectively.

Proof. If $sp \le 1$, then D = 1 is sufficient and we can use the bounds in [17][Theorem 2].

For sp > 1 we use the uniformly bounded implementation (see Section IV D). We now prove that it produces the desired logical error rate and gate overhead.

Let $\alpha = \frac{9(4A_V + 2B_V) + 3A_I}{2}$. From Lemma 5, a sufficient condition for a vanishing logical error rate at $np \to 0$ is that $(\alpha np)^{D-1} < 1/sp$, where we used the fact that α is a constant so $\alpha np \to 0$.

Setting $D = \log(sp) + 1$ the condition reduces to $\log(\alpha np) < -1$ which is satisfied since $\alpha np \to 0$.

The bound for the gate overhead from Lemma 6 is $\omega_{\rm G} \leq 2(12^D) < 24 \lceil (sp)^4 \rceil$. The qubit overhead is given in Proposition 1.

The condition $np \to 0$ cannot be avoided with CliNR since the logical error rate is always bounded from below by the logical error rate in RSI which has $A_I n$ noisy gates. On the other hand, the bound on ω_G is loose, e.g. it can be tightened to $\omega_G \leq 2$ when $snp^2 \to 0$ [17].

B. Notation

We continue to use the notation from Algorithm 1 unless stated otherwise. We use $r_{\ell,j} = \mathbf{r}(v_{\ell,j})$ and $s_{\ell,j} = \mathbf{s}(v_{\ell,j})$. Note that we only consider pairs \mathcal{T} , C such that $s_{0,0} = s$ is the size of C and $r_{0,0} = 0$.

We use $\mathcal{T}_{\ell,j}$ for a CliNR tree constructed by taking the subtree of \mathcal{T} consisting of the vertex $v_{\ell,j}$ and all its children, and setting $r_{0,0} = 0$.

We also use $\hat{s}_{\ell,j}$ to denote the expected number of gates in the implementation of CliNR($\mathcal{T}_{\ell,j}, C_{\ell,j}$), accounting for the repetitions due to the restarts in all RSV of the tree. We use $\hat{s}_{\ell} = \max_{j}(\hat{s}_{\ell,j})$.

The constants A_P , A_V , B_V , A_I are used to bound gate counts (as defined in Section IIB). We define $m_{\ell,j} = A_P n + r_{\ell,j} (A_V n + B_V)$, which we use to upper bound size of a single RSP+RSV iteration. When there is no risk of

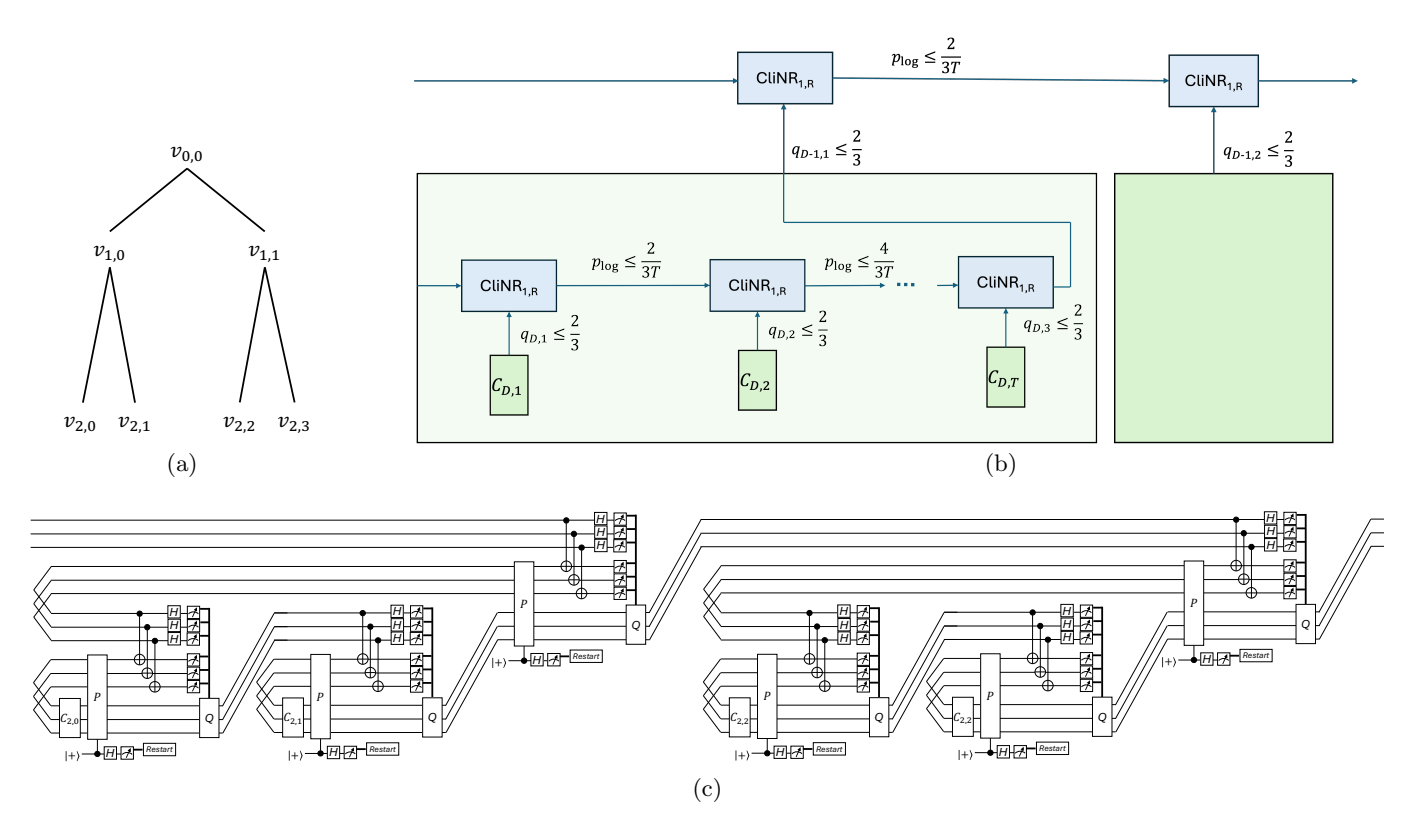


FIG. 2. Recursive CliNR. (a) A depth 2 CliNR tree. Each vertex in the tree has two associated parameters $\mathbf{r}(v_{\ell,j}) = r_{\ell,j}$ and $\mathbf{s}(v_{\ell,j}) = s_{\ell,j}$ referring to the number of stabilizer measurements and size of the subcircuit $C_{\ell,j}$. (b) Schematic for the uniformly bounded implementation of Recursive CliNR. Shown is only part of the implementation starting at the beginning of the circuit. Note that the *input state* for the first (bottom left) CliNR₁ block is determined by the previous level. The entire green block is the *input circuit* to the level above. The specific choice of tree parameters (based on s) ensures that the logical error rate at each input $(q_{\ell,j})$ and output (p_{\log}) state/circuit is bounded. Each implementation of CliNR_{1,R} has an input circuit with logical error rate of at most 2/3 and an output with logical error rate at most 2/3T. The total error is therefore upper bounded by $(2/3T)t_1$ where t_1 is the number of vertices at level 1. (c) Circuit implementation of Recursive CliNR with the tree from (a) and n=3. For simplicity $r_{\ell,j}=1$ for all $(\ell,j)\neq (0,0)$. Note that the same ancilla can be used for all stabilizer measurements. The total qubit count is 16.

confusion we use m instead of $m_{\ell,j}$. We also use upper and lower bars to denote the max and min of a variable over all vertices in the same level e.g. $\bar{r}_{\ell} = \max_{j}(r_{\ell,j})$ and $\underline{r}_{\ell} = \min_{j}(r_{\ell,j})$. We use the notation $g_p(x) = 1 - (1-p)^x$.

We use p_{\log} to denote the logical error rate in a specific context (usually for the CliNR implementation). In cases where confusion is possible we use an argument e.g. $p_{\log}(C) \leq g_p(s)$ is the logical error rate in the direct implementation of C.

For each vertex $v_{\ell,j}$ of \mathcal{T} , the subtree error rate, denoted $q_{\ell,j}$ is defined to be the logical error rate of the implementation $\text{CliNR}(\mathcal{T}_{\ell,j}, C_{\ell,j})$ of $C_{\ell,j}$. The logical error rate of the whole recursive implementation of C is equal to $q_{0,0}$. We use the notation $\bar{p}_{b\ell}$ for an upper bound on $\max_i q_{\ell,j}$.

An easy reference table for notation is provided in Table I of Section A.

C. Bounds on recursive CliNR

This section provides general bounds on the performance and the overhead of the recursive CliNR scheme, including the statements that lead to Theorem 1.

The following known result is used as the motivation for random stabilizer measurements.

Lemma 1. Let S_r be a set of r stabilizers selected independently and uniformly at random from a stabilizer group S. Let E be a Pauli operator that does not commute with S. The probability that E commutes with S_r is 2^{-r} .

Proof. Exactly half of the stabilizers in the group S commute with E, so each randomly selected stabilizer has a probability of 1/2 to commute with E. The probability that r randomly selected stabilizers all commute with E is therefore 2^{-r} .

Lemma 1 in [17] provides bounds for the performance of $CliNR_{1,r}$ when the input circuit has a fixed size. The

lemma below is a slight extension that explicitly allows the input circuit to have variable size with an expected size \hat{s} .

Lemma 2 (CliNR₁ bounds). The implementation CliNR_{1,r}(C) of an n-qubit Clifford circuit C with an expected size \hat{s} has logical error rate

$$p_{\log} \le \frac{\left(1 - (1 - p)^{A_P n} (1 - p_{\log}(C)) 2^{-r} + 2g_p(A_V n + B_V)\right)}{(1 - p)^m (1 - p_{\log}(C))} \tag{1}$$

$$+g_p(A_In)\cdot$$

Moreover, the gate overhead satisfies

$$\omega_{\mathcal{G}} \le \frac{(m+\hat{s})}{\hat{s}(1-p)^m \left(1-p_{\log}(C)\right)} + \frac{A_I n}{\hat{s}}.$$
 (2)

It is possible to implement $CliNR_{1,r}(C)$ using 3n + 1 qubits.

Proof. The fact that $CliNR_{1,r}(C)$ implements C and that it can be implemented with 3n+1 qubits is apparent from its structure. Note that the same ancilla can be re-used on all stabilizer measurements.

For $\omega_{\rm G}$, we need to bound the probability of a restart due to a stabilizer measurement. A necessary condition is an error before or during the stabilizer measurement. The probability of an error at any point in RSP and RSV is therefore an upper bound on the restart probability, so $p_{\rm res} \leq 1 - (1-p)^m (1-p_{\rm log}(C))$.

The expected number of times the repeating part of the circuit (RSP and RSV) is executed is upper bounded by

$$\sum_{k\geq 1} k p_{\text{res}}^{k-1} (1 - p_{\text{res}})$$

$$= \frac{1}{1 - p_{\text{res}}}$$

$$\leq \frac{1}{(1 - p)^m (1 - p_{\log}(C))}.$$

The total expected gate count is $\omega_{G}\hat{s} \leq \frac{(m+\hat{s})}{(1-p)^{m}(1-p_{\log}(C))} + A_{I}n$.

For a logical error at the output of CliNR₁ at least one of the the following three events must occur: (1) A logical error during RSP which is not detected during RSV (with probability p_{RSP}); (2) A logical error during a stabilizer measurement which is not detected by a subsequent stabilizer measurement (with probability p_{RSV}); (3) A logical error during RSI (with probability p_{RSI}).

The logical error rate is upper bounded by the sum of the probabilities for the events above, conditioned on the circuit not restarting,

$$p_{\log} \le \frac{p_{RSP} + p_{RSV}}{1 - p_{\text{res}}} + p_{RSI}. \tag{3}$$

(RSP) A logical error in RSP will not be detected during RSV if it commutes with all the stabilizer measurements. It might also not be detected due to an

error during RSV, but that is accounted for in p_{RSV} . The probability of a logical error in RSP is $1 - (1 - p)^{A_P n} (1 - p_{\log}(C))$. Using Lemma 1 we have $p_{RSP} \leq (1 - (1 - p)^{A_P n} (1 - p_{\log}(C)) 2^{-r}$

(RSV) The probability of an error during the ith stabilizer measurement is $1-(1-p)^{A_V n+B_V}$. The probability that it is a logical error which is also not detected by one of the latter stabilizer measurements is at most $(1-(1-p)^{A_V n+B_V}) 2^{-r+i}$. So

$$p_{RSV} \le \sum_{i=1}^{r} (1 - (1-p)^{A_V n + B_V}) 2^{-r+i} \le 2g_p(A_V n + B_V).$$

(RSI) At most $A_I n$ operations are required for RSI so $p_{RSI} \leq g_p(A_I n)$.

Plugging the bounds into Eq. (3) gives Eq. (1)

Lemma 3 (Logical error bounds for Recursive CliNR). Let \mathcal{T} be a CliNR tree of depth D. The implementation CliNR(\mathcal{T} , C) has a logical error rate

$$p_{\log} \leq t_1 \left(\frac{\left(1 - (1 - p)^{A_P n} (1 - \bar{p}_{b1})\right) 2^{-\underline{r}_1} + 2g_p (A_V n + B_V)}{(1 - p)^{\bar{m}_1} (1 - \bar{p}_{b1})} + g_p (A_I n) \right), \tag{4}$$

where

$$\bar{p}_{b\ell} = \bar{t}_{\ell+1} \Big((5) \\
\frac{\left(1 - (1-p)^{A_P} (1-\bar{p}_{b\ell+1})\right) 2^{-\underline{r}_{\ell+1}} + 2g_p(A_V n + B_V)}{(1-p)^{\bar{m}_{\ell+1}} (1-\bar{p}_{b\ell+1})} \\
+ g_p(A_I n) \Big),$$

for $\ell \leq D$, and

$$\bar{p}_{bD} = (1-p)^{\bar{s}_D}. \tag{6}$$

Proof. We do the proof by induction starting with D=1 as the base case. At D=1 we have a sequence of t_1 CliNR_{1, r_j}($C_{1,j}$). The upper bound of Eq. (4) is a consequence of adding the logical error rates from t_1 implementations, CliNR_{1, r_i}($C_{1,j}$), and using the bound in Lemma 2.

Assume that Eq. (4) holds for D=d and let us prove this bound for D=d+1. We start by constructing a CliNR tree \mathcal{T}^- , starting from \mathcal{T} and removing all vertices at level D. By hypothesis, Eq. (4) holds for CliNR(\mathcal{T}^-,C). The circuit CliNR(\mathcal{T},C) is constructed (see Algorithm 1) by first constructing the circuit CliNR(\mathcal{T}^-,C) and then replacing each subcircuit $C_{d,j}$ with a sequence of at most \bar{t}_d CliNR₁ circuits. Each of these have a logical error rate bounded by $\bar{p}_{bd}/\bar{t}_{d+1}$ (from Lemma 2), leading to Eq. (4).

Lemma 4 (Gate overhead for CliNR tree). Let \mathcal{T} be a CliNR tree of depth D. The gate overhead for the implementation $CliNR(\mathcal{T}, C)$ satisfies

$$\omega_{\rm G} \le \frac{\bar{t}_1}{s} \left(\frac{(\bar{m}_1 + \hat{s}_1)}{(1 - p)^{\bar{m}_1} (1 - \bar{p}_{b1})} + A_I n \right),$$
 (7)

where \bar{p}_{b1} is given by the recursive expressions in Eq. (5) and Eq. (6), and \hat{s}_1 is given by the recursive expression

$$\hat{s}_{\ell} \le \bar{t}_{\ell+1} \left(\frac{\bar{m}_{\ell+1} + \hat{s}_{\ell+1}}{(1-p)^{\bar{m}_{\ell+1}} (1-\bar{p}_{b\ell+1})} + A_I n \right) \tag{8}$$

for $\ell < D$, and \hat{s}_D is the size of the largest subcircuit at depth D.

Proof. We prove this by induction. For D = 1 (base case) we have a sequence of \bar{t}_1 implementations of $\operatorname{CliNR}_{1,r_{1,i}}(C_i)$ each with an upper bound on the expected gate number given by Lemma 2, leading to Eq. (7).

The induction hypothesis is that Eq. (7) holds for D=d. For D=d+1 we begin by constructing a CliNR tree \mathcal{T}^- starting from \mathcal{T} and removing all vertices at level D. By hypothesis, Eq. (7) holds for $CliNR(\mathcal{T}^-, C)$. The $CliNR(\mathcal{T}, C)$ circuit is constructed by first constructing $CliNR(\mathcal{T}^-, C)$ and then replacing each subcircuit $C_{d,j}$ with a sequence of at most \bar{t}_{d+1} CliNR₁ circuits (see Algorithm 1). Each of these $CliNR_1(C_{D,j})$ circuits has an expected gate count with an upper bound given in Lemma 2. Multiplying the largest of these by \bar{t}_{d+1} gives Eq. (7).

Uniformly bounded implementation

To prove Theorem 1, we introduce a new class of recursive CliNR implementations which we call uniformly bounded (see Fig. 2 b). Before going to a formal definition, we provide some intuition by listing a few properties which are valid at the limit $np \to 0$ (see proof of Lemma 5 and Theorem 1).

- 1. For each implementation of CliNR₁, the logical error rate in RSP is similar to the logical error rate in RSV, i.e. the two terms in the numerator of Eq. (5) have a similar value (of order np).
- 2. There is a bounded subtree error $q_{\ell,r} < 2/3$ for all $\ell > 1$.
- 3. The logical error rate $q_{0,0} < O(sn^D p^{D+1})$.
- 4. The logical error rate $q_{0,0}$ vanishes when D = $\max(1, \log(sp)).$

Property 1 means that the logical error at the output of each $CliNR_1$ block is independent of s. Intuition on property 2 and how it leads to 3 given in Fig. 2 (b). Property 4 follows from 3 (Theorem 1).

Definition 1 (Uniformly bounded CliNR). A Uniformly bounded CliNR implementation with depth D, is a recursive CliNR implementation using a CliNR tree constructed using Algorithm 2.

For the purposes of the algorithm we define the following functions

$$T(p,n) := \left| \frac{2}{9(4A_V n + 2B_V)p + 3A_I np} \right| \tag{9}$$

and

$$R(p,n) := \lceil \log \left(pA_P n \left(1 - \frac{2}{3} \right) + \frac{2}{3} \right) - \log(2A_V n p)) \rceil. \tag{10}$$

We say that $\mathcal{T}(\mathbf{s}, \mathbf{r})$ is empty if it has no vertices and the functions **s** and **r** map all vertices $v_{\ell,j}$ to 0.

Algorithm 2: Algorithm for constructing a CliNR tree for a uniformly bounded implementation

input: A n-qubit Clifford circuit C with size s. A noise parameter p.

output: A CliNR tree \mathcal{T} .

- 1 Let R = R(p, n), and T = T(p, n).
- 2 Create an empty tree $\mathcal{T} = \mathcal{T}(\mathbf{s}, \mathbf{r})$. All vertices added below are for \mathcal{T} .
- 3 Set $t' = \left\lceil \frac{3sp}{2} \right\rceil$
- **4** Add vertices $v_{D,j}, j \in \{0, ..., t'-1\}$.
- 5 for $j \in \{0, \dots, (s \mod t') 1\}$ do
- $\int \mathbf{set} \mathbf{s}(v_{D,j}) = \begin{bmatrix} \frac{s}{t'} \end{bmatrix}.$
- 7 for $j \in \{s \mod t', \dots, t'-1\}$ do 8 $\lfloor \operatorname{set} \mathbf{s}(v_{D,j}) = \lfloor \frac{s}{t'} \rfloor$.
- 9 for $\ell \in \{D-1, ..., 1\}$ do
- Set k = 0. 10 **while** there are vertices in layer $\ell + 1$ with no 11
- parent in layer ℓ do Let V be the set of first T vertices in layer 12
- $\ell + 1$ with no parent. Add vertex $v_{\ell,k}$. 13
- Make all vertices in V children of $v_{\ell,k}$. **14**
- Set $\mathbf{s}(v_{\ell,k}) = \sum_{v \in V} \mathbf{s}(v)$. Set k = k + 1. 15
- 16
- 17 For all vertices $v_{\ell,j} \in \mathcal{T}$, set $\mathbf{r}(v_{\ell,j}) = R$.
- **18** Add vertex $v_{0,0}$ and set $\mathbf{s}(v_{0,0}) = s$, and $\mathbf{r}(v_{0,0}) = 0$.
- 19 Make all vertices at level one children of $v_{0,0}$.
- 20 return \mathcal{T} .

The following properties are a direct consequence of Algorithm 2.

Proposition 2. The uniformly bounded implementation of a Clifford circuit with s > 1/p has the following prop-

- $C_{D,j}$ are of size at most $\bar{s}_D = \frac{2}{3p}$ and at least $\frac{1}{2p}$.
- The CliNR tree has $\lceil \frac{s}{\bar{s}_D} \rceil$ vertices at level D.

- Each vertex $v_{\ell,j}$ with $D > \ell > 0$ has at most t = T(p,n) children.
- $r_{\ell,j} = R(p,n)$ for all $\ell \neq 0, j$.

Lemma 5 (Logical error rate for a uniformly bounded implementation). If $A_P n + 2R(p,n)(A_V n + B_V) + A_I n < 1/(2p)$ then a uniformly bounded CliNR implementation with depth D has a logical error rate

$$p_{\log} \le sp^{D+1} \left(\frac{9(4A_V n + 2B_V) + 3A_I n}{2} \right)^D$$
 (11)

Proof. For a uniformly bounded implementation, the number of children for $v_{0,0}$ is $t_1 \leq \left\lceil \frac{s}{\bar{s}_D t^{D-1}} \right\rceil$. The value of all $m_{\ell,j}$ is fixed and denoted m.

Using Lemma 3, our aim is to prove that $\bar{p}_{b\ell}$ in Eq. (5) remains bounded for all $\ell > 1$. We do this by first assuming that $\bar{p}_{b\ell+1} \leq 2/3$ and then proving that this assumption is true for all ℓ .

Using the Bernoulli bound $(1-p)^x \ge (1-xp)$ in Eq. (5) gives,

$$p_{b\ell} \leq \bar{t}_{\ell+1} \left((12) \frac{(A_P n p (1 - \bar{p}_{b\ell+1}) + \bar{p}_{b\ell+1}) 2^{-r} + 2(A_V n + B_V) p}{(1 - m p) (1 - \bar{p}_{b\ell+1})} + A_I n p \right).$$

Since $r = \lceil \log(pA_P n(1-2/3) + 2/3) - \log(2A_V np)) \rceil$ and assuming $\bar{p}_{b\ell+1} \le 2/3$ gives

$$p_{b\ell} \le \bar{t}_{\ell+1} \left(\frac{(4A_V n + 2B_V)p}{(1 - mp)(1 - \bar{p}_{b\ell+1})} + A_I np \right).$$

By assumption 1-mp>1/2, and by construction $\bar{t}_{\ell+1}<\frac{2}{9(4A_Vn+2B_V)p+3A_Inp}$ so if $\bar{p}_{b\ell+1}\leq 2/3$ we have $p_{b\ell}\leq 2/3$. Since $p_{bD}<2/3$ is ensured from $\bar{s}_Dp\leq 2/3$ then our assumption $p_{b\ell}\leq 2/3$ is guaranteed to be true for all $\ell\geq 1$.

The same can be done for Eq. (4) replacing t with t_1 so $p_{\log} \leq \frac{2}{3} \frac{t_1}{t} \leq sp \left(\frac{9(4A_V n + 2B_V)p + 3A_I np}{2} \right)^D$.

Note that at D=1 we recover the snp^2 scaling obtained in [17]. When D>1, we get $p_{\log} \leq O(sn^Dp^{D+1})$.

Lemma 6 (Gate overhead for for a uniformly bounded implementation). Under the same conditions as Lemma 5, ω_G for CliNR($\mathcal{T}^{B,D}$, C) satisfies

$$\omega_{\rm G} < 2(12^D)$$
.

Proof. Starting with the bounds on $\omega_{\rm G}$ in Lemma 4 and plugging $p_{b\ell} < 2/3$ in Eq. (8), together with the condition mp < 1/2 and the Bernoulli bound we get,

$$\hat{s}_{\ell} \leq t \left(6(m + \hat{s}_{\ell+1}) + A_I n \right).$$

We also have $\bar{s}_D \leq \frac{2}{3p}$ by construction. By assumption $m+A_In < \frac{1}{2p}$ reducing the expression to

$$\hat{s}_{\ell} \le t \left(6 \left(\frac{1}{2p} + \hat{s}_{\ell+1} \right) \right).$$

This implies $\hat{s}_{\ell} \leq 12\hat{s}_{\ell+1}$ since $\hat{s}_{\ell+1} \geq \frac{1}{2p}$. We then get $\omega_{\mathrm{G}} s \leq 12t_1(12t)^{D-1}\bar{s}_D \leq 12^D2s$. Where in the last step we used $t_1 \leq \left\lceil \frac{s}{\bar{s}_D t^{D-1}} \right\rceil$.

V. NUMERICAL RESULTS

To show the advantage of Recursive CliNR in experimentally relevant regimes we use two different techniques: A fast Markov model technique (see Section B 1) and a Monte Carlo simulation. The Markov model (based on [6]) works by tracking the probabilities of errors and stabilizer measurement outcomes through the circuit. It is significantly faster than the simulation (built using Stim [19]), but also less accurate (see Fig. 6 in Section C). In both cases we consider the circuit level noise model with error rate p for two-qubit gates, p/10 for single-qubit operations (gate and measurements) and either p/1000 for idle qubits or no idle errors. The errors are depolarizing for qubits and bit-flip for measurements.

For the simulation, we use $p = 10^{-3}$. For the Markov model we use both $p = 10^{-3}$ and 10^{-4} and supplement the error model with estimated parameters given in Section B 3. Results are shown in Fig. 3 (Markov model) and Fig. 4 (Simulation).

The values were chosen based on existing results for trapped ions. One and two qubit errors below 0.002% and 0.01% respectively have been demonstrated with trapped ions [20, 21]. Ion qubit coherence times of $T_2^* > 1000$ seconds have been demonstrated [22], and theoretical results predict fast two gates for trapped ions on the order of a microsecond [23]. At these gate speeds and T_2^* , the idle error rate should be lower than 10^{-9} .

The advantages of Recursive CliNR are expected to be more pronounced for large circuits. We therefore studied the family of circuits that has the largest expected gate-count (for given n), *i.e.* random Clifford circuits, making slight adjustments (either trimming or padding) so that the gate count is fixed at n^2 .

A. Estimated performance

Using the Markov model (Section B 1) we searched for values of n where Recursive CliNR at depth 2 will outperform the standard CliNR scheme (i.e. Recursive CliNR

at depth 1). Results presented here are for 70 qubits at $p=10^{-3}$ with idle noise (Fig. 3 (a)) and 400 qubits at $p=10^{-4}$ with no idle noise (Fig. 3 (b)). We considered trees with different numbers of vertices at $\ell=1$ (ranging from 1 to 10), each having the same number of children (0 for D=1, and 2 to 10 for D=2). Each tree had a fixed $r_{\ell,j}=r$ for $\ell\neq 0$. We used r ranging from 0 to 30.

The plots (Fig. 3) show the Pareto frontier (best $\omega_{\rm G}$, $p_{\rm log}$ values) at each depth with a cutoff for the overhead, $\omega_{\rm G} \leq 100$. We note that if we allow arbitrarily large $\omega_{\rm G}$, it is possible to reach much lower logical error rates at both depth 1 and depth 2.

The results of the estimates should be used as a guide for showing relative performance qualitatively, and for finding good tree parameters. The precision drops as the overhead increases but improves when there is no idle noise. These limitations are discussed in Section C.

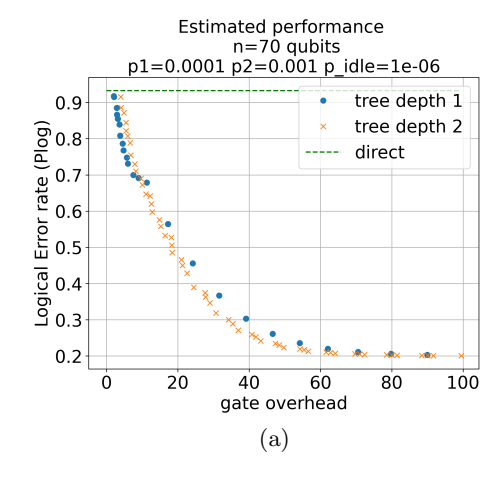
At n=70 (Fig. 3 (a)) we see that Recursive CliNR has a significant advantage at around $\omega_{\rm G}=21$, providing a guide for points we want to simulate (Fig. 4). At n=400, Fig. 3 (b) shows a significant advantage for the depth 2 tree starting at around $\omega_{\rm G}=10$. We also see that logical error rates plateau at various points both at depth 1 and 2 and then start improving again. Escaping the plateau requires a tree with fewer vertices, the cost is a (usually significant) increase in gate overhead. We note that this continues at larger overheads (not shown) and that both depth 1 and 2 seem to have the same performance at very large $\omega_{\rm G}$.

B. Numerical simulations

We used Stim [19] to run Monte Carlo simulations. These included a complete run of the circuit with all restart events. Random Cliffords were generated using Qiskit [24] with some padding or truncation of the generated circuit so that the gate count is fixed at n^2 . Each data point in Fig. 4 is the average over 50 different Clifford input circuits, each with 80 shots. The input state was always $|0\rangle^{\otimes n}$. Error bars are the standard deviation over the 50 different circuits.

Using the Markov model, we were unable to identify an advantage for Recursive CliNR at n < 100 and $p = 10^{-4}$. Consequently we set $p = 10^{-3}$ and n = 70 to keep the simulation time manageable. Results are plotted in Fig. 4 and compared to the estimates of the previous section in Section C. Specific data points were chosen by using the Markov model to generate a Pareto frontier and taking points where $\omega_{\rm G} \leq 21$.

The results show a similar trend to the estimates in Fig. 3. When there is no idle noise, we clearly see the advantage of using depth 2 trees (i.e. Recursive CliNR) starting at $\omega_{\rm G} \approx 15$. With idle noise, the advantage is less obvious due to inaccuracies introduced by choosing points with the Markov model (see Fig. 6). Nevertheless, we can see the improvement in depth 2 at the larger values of $\omega_{\rm G}$ as predicted in Fig. 3 (a). We also see the



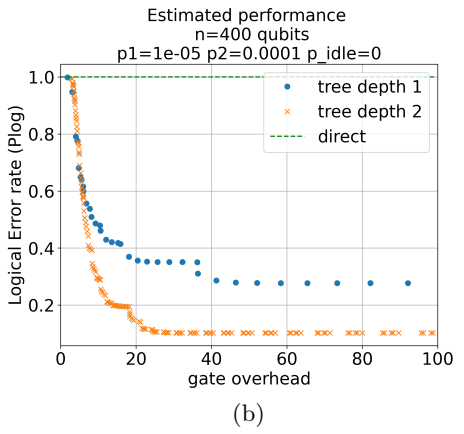


FIG. 3. Numerical estimates of the performance based on the Markov model at (a) $n=70, p=10^{-3}$ and (b) $n=400, p=10^{-4}$ with no idle noise. In both cases the gate overhead was capped at $\omega_{\rm G}<100$. Plotted points are the Pareto frontiers at depth 1 and 2. Note that the performance estimates tend to be less accurate when the gate overheads are large but the trend remains indicative (see Section C). Results for n=70 can be compared with direct simulation in Fig. 4. Results for n=400 show a significant advantage when going to depth 2, e.g. at a gate overhead of $\omega_{\rm G}\approx25.5$ we have $p_{\rm log}\approx0.35$ at depth 1 and $p_{\rm log}\approx0.10$ at depth 2.

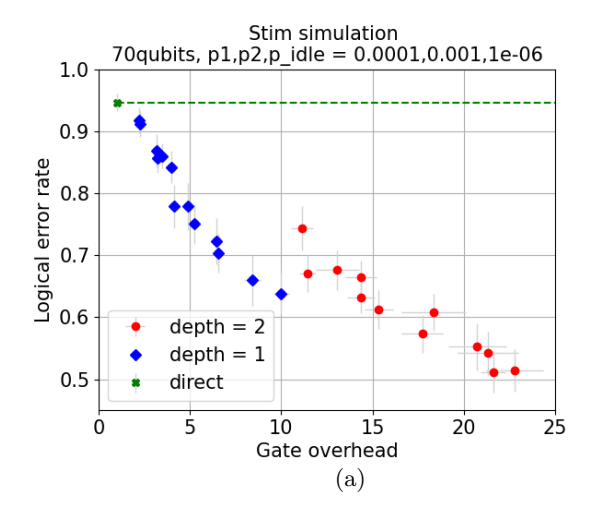
impact of idle noise when comparing Fig. 4 (a) to (b).

A comparison of the Stim simulation and the Markov method estimates is given in Section C.

VI. CONCLUSIONS

Our main result shows that Recursive CliNR can be used to reduce the logical error rate of any size circuit to an arbitrarily low value when $np \to 0$. This result can be compared with the asymptotic bound $snp^2 \to 0$ for the original CliNR. For the largest Clifford circuits (of order $n^2/\log(n)$) [25]) the condition for CliNR₁ becomes $(n^3p^2)/\log(n) \to 0$ compared to $np \to 0$ for Recursive CliNR.

Our numerical results show that in-practice (assuming



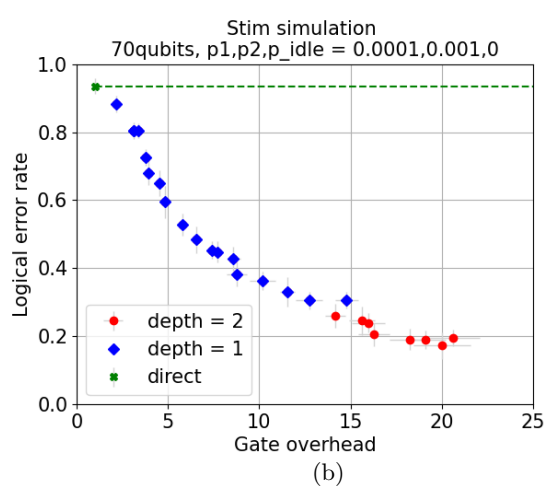


FIG. 4. Simulation results at n=70 and $p=10^{-3}$. (a) With idle noise; (b) Without idle noise. Results are capped at $\omega_{\rm G} < 21$. In both cases we see the trend predicted in Fig. 3 as we move from depth 1 (blue diamonds) to depth 2 (red circles). The direct implementation is given as a reference (green dashed line).

realistic physical error rates and near-term qubit counts) the main advantage of the recursive scheme is at fixed gate overheads. Recursive CliNR can have lower logical error rates when we limit $\omega_{\rm G}$. The advantage is particularly pronounced when the idle errors are very small, a feat that is achievable for trapped ion qubits.

If more qubits are available, it is possible to parallelize operations, in particular the sequential implementation of CliNR₁ blocks at the same depth. We did not study this regime but we expect it to lead to significant improvements in running time, and a significant reduction in idle time. Additionally it is possible to carefully select the stabilizers as in [18] and reduce the overheads in RSV which would subsequently reduce idle time.

In the near-term we expect CliNR, Recursive CliNR and similar schemes to play an important role in quantum computing. Enabling algorithms with circuits that may be deep enough for so-called utility-scale quantum computing without full blown error correction. In the longer term it is likely that these types of schemes will still play a role in conjunction with QEC, maximizing resource efficiency.

VII. ACKNOWLEDGMENT

The authors thank Felix Tripier, Andy Maksymov, Min Ye, John Gamble and the whole IonQ team for insightful discussions.

^[1] D. Aharonov and M. Ben-Or, Fault-tolerant quantum computation with constant error, in *Proceedings of the twenty-ninth annual ACM symposium on Theory of computing* (1997) pp. 176–188.

^[2] P. Aliferis, D. Gottesman, and J. Preskill, Quantum accuracy threshold for concatenated distance-3 codes, arXiv preprint quant-ph/0504218 (2005).

^[3] D. Litinski, Magic state distillation: Not as costly as you think, Quantum 3, 205 (2019).

^[4] S. Bravyi, A. W. Cross, J. M. Gambetta, D. Maslov, P. Rall, and T. J. Yoder, High-threshold and lowoverhead fault-tolerant quantum memory, Nature 627, 778 (2024).

^[5] C. Gidney, How to factor 2048 bit rsa integers with less than a million noisy qubits (2025), arXiv:2505.15917 [quant-ph].

^[6] T. J. Yoder, E. Schoute, P. Rall, E. Pritchett, J. M. Gambetta, A. W. Cross, M. Carroll, and M. E. Beverland, Tour de gross: A modular quantum computer based on bivariate bicycle codes (2025), arXiv:2506.03094 [quantph].

^[7] F. Arute, K. Arya, R. Babbush, D. Bacon, J. C. Bardin, R. Barends, R. Biswas, S. Boixo, F. G. Brandao, D. A. Buell, et al., Quantum supremacy using a programmable superconducting processor, Nature 574, 505 (2019).

^[8] M. DeCross, R. Haghshenas, M. Liu, E. Rinaldi, J. Gray, Y. Alexeev, C. Baldwin, J. Bartolotta, M. Bohn, E. Chertkov, J. Cline, J. Colina, D. DelVento, J. Dreiling, C. Foltz, J. Gaebler, T. Gatterman, C. Gilbreth, J. Giles, D. Gresh, A. Hall, A. Hankin, A. Hansen, N. Hewitt, I. Hoffman, C. Holliman, R. Hutson, T. Jacobs, J. Johansen, P. Lee, E. Lehman, D. Lucchetti, D. Lykov, I. Madjarov, B. Mathewson, K. Mayer,

- M. Mills, P. Niroula, J. Pino, C. Roman, M. Schecter, P. Siegfried, B. Tiemann, C. Volin, J. Walker, R. Shaydulin, M. Pistoia, S. Moses, D. Hayes, B. Neyenhuis, R. Stutz, and M. Foss-Feig, Computational power of random quantum circuits in arbitrary geometries, Physical Review X 15, 10.1103/physrevx.15.021052 (2025).
- [9] A. e. a. Morvan, Phase transitions in random circuit sampling, Nature **634**, 328–333 (2024).
- [10] Z. Zimborás, B. Koczor, Z. Holmes, E.-M. Borrelli, A. Gilyén, H.-Y. Huang, Z. Cai, A. Acín, L. Aolita, L. Banchi, F. G. S. L. Brandão, D. Cavalcanti, T. Cubitt, S. N. Filippov, G. García-Pérez, J. Goold, O. Kálmán, E. Kyoseva, M. A. C. Rossi, B. Sokolov, I. Tavernelli, and S. Maniscalco, Myths around quantum computation before full fault tolerance: What no-go theorems rule out and what they don't (2025), arXiv:2501.05694 [quantph].
- [11] Z. Cai and S. C. Benjamin, Constructing smaller pauli twirling sets for arbitrary error channels, Scientific Reports 9, 11281 (2019).
- [12] D. M. Debroy and K. R. Brown, Extended flag gadgets for low-overhead circuit verification, Physical Review A 102, 052409 (2020).
- [13] E. van den Berg, S. Bravyi, J. M. Gambetta, P. Jurcevic, D. Maslov, and K. Temme, Single-shot error mitigation by coherent pauli checks (2022), arXiv:2212.03937 [quant-ph].
- [14] J.-S. Chen, E. Nielsen, M. Ebert, V. Inlek, K. Wright, V. Chaplin, A. Maksymov, E. Páez, A. Poudel, P. Maunz, and J. Gamble, Benchmarking a trapped-ion quantum computer with 30 qubits, Quantum 8, 1516 (2024).
- [15] I. A. Chernyshev, R. C. Farrell, M. Illa, M. J. Savage, A. Maksymov, F. Tripier, M. A. Lopez-Ruiz, A. Arrasmith, Y. de Sereville, A. Brodutch, C. Girotto, A. Kaushik, and M. Roetteler, Pathfinding quantum simulations of neutrinoless double-β decay (2025), arXiv:2506.05757 [quant-ph].
- [16] J. Roffe, D. Headley, N. Chancellor, D. Horsman, and V. Kendon, Protecting quantum memories using coherent parity check codes, Quantum Science and Technology 3, 035010 (2018).
- [17] N. Delfosse and E. Tham, Low-cost noise reduction for clifford circuits, arXiv preprint arXiv:2407.06583 (2024).
- [18] E. Tham and N. Delfosse, Optimized clifford noise reduction: Theory, simulations and experiments (2025), arXiv:2504.13356 [quant-ph].
- [19] C. Gidney, Stim: a fast stabilizer circuit simulator, Quantum 5, 497 (2021).
- [20] C. M. Löschnauer, J. M. Toba, A. C. Hughes, S. A. King, M. A. Weber, R. Srinivas, R. Matt, R. Nourshargh, D. T. C. Allcock, C. J. Ballance, C. Matthiesen, M. Malinowski, and T. P. Harty, Scalable, high-fidelity all-electronic control of trapped-ion qubits (2024), arXiv:2407.07694 [quant-ph].
- [21] A. Hughes, R. Srinivas, C. Löschnauer, H. Knaack, R. Matt, C. Ballance, M. Malinowski, T. Harty, and R. Sutherland, Trapped-ion two-qubit gates with; 99.99% fidelity without ground-state cooling, arXiv preprint arXiv:2510.17286 (2025).
- [22] P. Wang, C.-Y. Luan, M. Qiao, M. Um, J. Zhang, Y. Wang, X. Yuan, M. Gu, J. Zhang, and K. Kim, Single ion qubit with estimated coherence time exceeding one hour, Nature Communications 12, 10.1038/s41467-020-20330-w (2021).

- [23] Z. Mehdi, V. D. Vaidya, I. Savill-Brown, P. Grosser, A. K. Ratcliffe, H. Liu, S. A. Haine, J. J. Hope, and C. R. Viteri, Fast mixed-species quantum logic gates for trappedion quantum networks (2025), arXiv:2412.07185 [quantph].
- [24] S. Bravyi and D. Maslov, Hadamard-free circuits expose the structure of the clifford group, IEEE Transactions on Information Theory 67, 4546–4563 (2021).
- [25] S. Aaronson and D. Gottesman, Improved simulation of stabilizer circuits, Physical Review A 70, 10.1103/physreva.70.052328 (2004).

Appendix A: Notation

This appendix can be used as a reference for notation introduced in the paper (mostly in Section IVB). The following general convention are used throughout the paper.

- Maximum over a set is indicated by a bar as in $\bar{r}\ell = \max_{j}(r_{\ell,j})$
- Minimum over a set is indicate by an underline as in $\underline{r}_{\ell,j} = \min_{j}(r_{\ell,j})$

Table I below indicates specific notation

Notation	Meaning	Notes
$\mathcal{T}_{\ell,j}$	Subtree of \mathcal{T}	See Section IV B
$C_{\ell,j}$	Clifford subcircuit	See Algorithm 1
$s_{\ell,j}$	Size of $C_{\ell,j}$	$\mathbf{s}(v_{\ell,j})$ in Algorithm 1,
,,,	- 12	$s = s_{0,0}$
\bar{s}_ℓ	$\max_j(s_\ell)$	
\underline{s}_{ℓ}	$\min_j(s_{\ell,j})$	
$rac{\underline{s}_{\ell}}{\hat{s}_{\ell,j}}$	The expected number of gates	
	in the implementation of	
	$\operatorname{CliNR}(\mathcal{T}_{\ell,j}, C_{\ell,j})$	
\hat{s}_ℓ	$\max_j(\hat{s}_{\ell,j})$	
$r_{\ell,j}$	Number of	$\mathbf{r}(v_{\ell,j})$ in Algorithm 1
	stabilizer measurements $v_{\ell,j}$	
$ar{r}_\ell$	$\max_j(r_{\ell,j})$	
\underline{r}_ℓ	$\min_j(r_{\ell,j})$	
$A_P, A_V,$	Constants used to	Independent of
		n, p, and s
B_V, A_I	bound gate counts	
$m_{\ell,j}$	$A_P n + r_{\ell,j} (A_V n + B_V)$	no subscript for CliNR ₁
$ar{m}_\ell$	$\max_j(m_\ell)$	
$g_p(x)$	$1 - (1 - p)^x$	
p_{\log}	logical error rate	$p_{\log}()$ with argument
		if context is necessary
$q_{\ell,j}$	Subtree error rate	As in Fig. 2
$ar{p}_{b\ell}$	Upper bound on $\max_j q_{\ell,j}$.	May not be tight
$\omega_{ m G}$	Gate overhead	
$\omega_{ m Q}$	Qubit overhead	

TABLE I. Notation

Appendix B: Optimizing the tree structure

Our aim is to provide practical methods for optimizing the tree parameters. In particular, we are interested finding a good solution to the following task: Given an input circuit C and a noise model, find a tree that optimized the values of p_{\log} and $\omega_{\rm G}$ in the Recursive CliNR implementation. Here optimal means that the results are on the Pareto frontier. In practice, we would usually also want to bound the gate overhead (e.g. $\omega_{\rm G} \leq 100$ in Fig. 3). The methods below are heuristic and are expected to provide close to optimal solutions.

Naively, one can simulate performance for different tree parameters and search for those that provide the best performance. In practice, the number of possible tree parameters is large, and Monte Carlo simulations such as those used in Section VB are relatively slow. The Markov model below is less accurate than a simulation (see Section C) but is significantly faster. It can be used to narrow down the search space.

1. Markov model and transition matrices

We use a modification of the Markov model introduced in [13] and a simplified error and circuit model to estimate errors at each stage.

The Markov model uses transition matrices to update a probability vector. We use the notation $T_{j,k}$ to denote the entry in the jth row and kth column of a transition matrix T. We start with estimating performance for $CliNR_{1,r}$ and then show how the model can be modified for recursive CliNR.

The Markov model works by propagating a vector \vec{P} of length r+3 that represents the probabilities for various events: \vec{P}_0 , no error; \vec{P}_1 , undetected error; and \vec{P}_{k+2} , detection at stabilizer measurement $k \in \{0, \ldots, r-1\}$.

The RSP probability vector: We denote p_p as the logical error rate for RSP. The state \vec{P} after RSP has $\vec{P}_0 = 1 - p_p$, $\vec{P}_1 = p_p$ and 0 for all other entries.

The RSV transition matrices: We use the stochastic matrix T(k) defined below to propagate \vec{P} through the k^{th} stabilizer measurement. $T_{00}(k) = 1 - p_{de} - p_{ue}$ where p_{de} and p_{ue} are the probabilities for errors during the stabilizer measurement (including measurements faults) that will be detected or undetected respectively. Similarly $T_{k+2.0}(k) = p_{de}$ and $T_{10} = p_{ue}$.

If there are no errors during the stabilizer measurement, the probability that a previously undetected error will be detected is 1/2, so $T_{1,1}(k) = 1/2$, $T_{k+2,1}(k) = 1/2$. We also have $T_{j,j}(k) = 1$ for all j > 1.

The RSI transition matrix: we can use a similar matrix W to propagate through RSI. Setting p_I as the logical error probability of RSI we have $W_{00} = 1 - p_I$, $W_{10} = p_I$ and $W_{k,k} = 1$ for all k > 0.

Calculating p_{\log} and ω_{G} : The logical error rate p_{\log} ' following this process is calculated using $p_{\log}' = \frac{\vec{P}_{1}}{\vec{P}_{0} + \vec{P}_{1}}$.

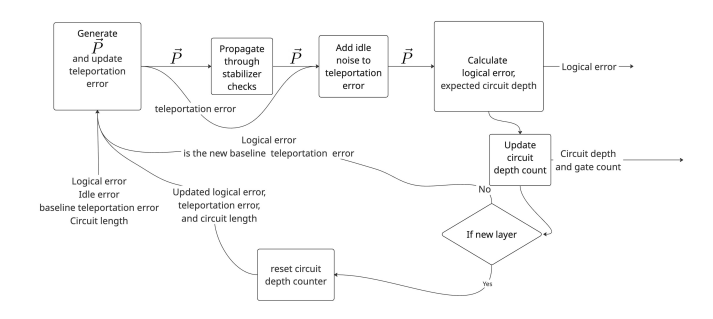


FIG. 5. Estimating the logical error rate and gate overhead. The probability vector \vec{P} is initialized with parameters from RSP and propagated through the stabilizer measurements (RSV). Idle noise on the input rails is accounted for during RSI and the logical error rate and expected gate count are calculated. The process is then repeated for the next CliNR block. At each new level we reset the depth-counter and update the expected depth of the input circuit.

Gate count: If we have g_P gates for RSP, g_C gates for each stabilizer measurement with r' stabilizer measurements and g_I gates for for RSI then the expected total number of gates executed is given by

$$g_{tot} = g_P + r'g_C + g_I + \sum_k (g_P + kg_P)m_{res(k)}$$
 (B1)

where $m_{\text{res}(k)}$ is the expected number of restarts at the k^{th} stabilizer measurement, $m_{\text{res}(k)} = \frac{\vec{P}_{k+2}}{p_{\text{res}}} \left(\frac{1}{1-p_{\text{res}}} - 1 \right)$ and $p_{\text{res}} = \sum_{k} \vec{P}_{k+2}$.

Recursive CliNR: For Recursive CliNR we propagate the vector through the circuit, re-initializing \vec{P} after each RSI step. We use the logical error rate calculated in the previous implementation, p_{\log} , to update the injection error p_I in a way that depends on the error model (see below) and specifically also accounts for idle errors.

The last step makes it easy to account for idle errors on the input rail (which can have significant impact). When we go one level up we set $\vec{P}_0 = 1 - p_{\log}'$ and $\vec{P}_1 = p_{\log}'$ and follow the same procedure (see Fig. 5).

2. Implementing different error models

The error model depends on two main factors. The implementation of each stage (e.g. the gate-set, connectivity, parallel operations) and the noise sources. Our aim is to provide values for p_p , p_{de} , p_{ue} and p_I , noting that these (in particular p_p and p_I) change as we go through the different instances of CliNR₁. This is because p_I depends on the input state which becomes more noisy as we go through implementations at the same level, and p_p depends on the input circuit which becomes more noisy as we go up levels.

The preparation and verification errors p_p , p_{de} , p_{ue} need to account only for the qubits in the resource state.

The RSI error, p_I , includes all errors in the input rails, including p_{\log} from the previous circuit, and any idling errors during execution. The idling errors are particularly sensitive to the expected size of the circuit which depends on the detection probabilities \vec{P}_{k+2} (see Section C).

3. Example

We consider the circuit level noise model with error rate p for two-qubit gates, p/10 for single-qubit operations (gate and measurements) and either p/1000 for idle qubits or no idle noise. The errors are depolarizing for qubits and bit-flip for measurements.

We also use the following approximations which are derived from averages over numerical data. The level-D subcircuits $C_{D,j}$ of size s' have s'/2 two-qubit gates and s'/2 single-qubit gates; The total number of single-qubit and two-qubit gates for RSP are s'/2 + 2n single-qubit gates and s'/2 + n two-qubit gates; The main source of idle errors is from qubits not participating in $C_{D,j}$ and the number of idle gates (in RSP) is $g_{Pidle} = s'n/3$.

The error rate for RSP is

$$p_p = 1 - (1-p)^{s'/2+n} (1-p/10)^{s'/2+2n} (1-p/1000)^{s'n/3}.$$

At levels above D we have

$$p_p = 1 - (1 - p_{\log}')(1 - p)^n (1 - p/10)^{2n} (1 - p/1000)^{\hat{s}'}$$

where \hat{s}' is the expected gate count for all children (calculated as part of the estimation algorithm and extended to account for idle errors).

For RSV we assume that each stabilizer measurement requires 6n/4 two-qubit gates (A random controlled 2n qubit Pauli implemented using a sequence of controlled X, Y or Z), two single-qubit gates and a measurement. There are 15 different two-qubit errors but one has no impact (X error on an X eigenstate), eight impact the measurement of the ancilla (detectable errors) and six do not. So

$$p_{de} = 1 - (1 - 8p/15)^{2n/3} (1 - 2p/30)^2 (1 - p/10),$$

and

$$p_{ue} = 1 - (1 - 6p/15)^{2n/3}.$$

For simplicity we derived an expression with no idle errors. These can be added using the same methodology.

For RSI we have a total of n two-qubit gates and 4n single-qubit gates or measurements. We assume that we minimize idling errors by timing the first operation in every branch correctly. When multiple CliNR₁ circuits feed into the same parent (i.e the corresponding $v_{\ell,j}$ have the same parent $v_{\ell-1,j'}$) then the first of these operations will have

$$p_I = 1 - (1 - p)^n (1 - p/10)^{4n}.$$

Subsequent rounds must also account for idle errors. We can use the same reasoning used to derive Eq. (B1). At level D the idle gate number from RSP remains $g_{Pidle} = s'n/3$. At each stabilizer measurement we have

$$(6n/4)(3n-2) = 4.5n^2 - 3n$$

idle gates so the expected total number of idle gates is

$$g_{idle} = \frac{s'n}{3} + r'(4.5n^2 - 3n)$$

$$+ \sum_{k} \left(\frac{s'n}{3} + k(4.5n^2 - 3n) \right) m_{\text{res}(k)}.$$
(B2)

Finally

$$p_I \approx 11 - (1-p)^n (1-p/10)^{4n} (1-p/1000)^{g_{idle}}$$
.

Note that this is an approximation that requires $g_{idle}p/1000 \ll 1$.

At levels above D we replace the s' by the expected gate count \hat{s}' .

4. Optimizing the tree

As noted previously, our aim is to find the optimal tree. This can be done by first itterating over a very large number of tree parameters using the Markov method and finding the Pareto frontier (as in Fig. 3). Once we identify a good parameter range, we can use slower, but more accurate method to find the best tree parameters around that range.

Appendix C: Analysis of the numerical estimates

The Markov method introduced in Section B1 is expected to provide an estimate of the logical error rates and gate overheads which can be used in parameter selection. The use of various approximations in the error parameters is expected to lead to small deviations. The small deviations can compound as the tree becomes deeper, leading to less accurate results at larger D. Below we compare the results of the Markov model to the results form the stabilizer simulation (see Section V B).

Fig. 6 shows the comparison between the two methods with and without idle noise. In both cases the parameters are $p = 10^{-3}$ and n = 70. All other parameters are chosen as in Section V.

Results with no idle noise Fig. 6 (a), (b) have good agreement between the two methods. When idle noise is added, Fig. 6 (c), (d), the logical error rates are still in good agreement, but the overhead estimates using the Markov method are consistently lower than the simulation when the values are high. The error bars in simulation are also much larger when $\omega_{\rm G}$ is large.

In all cases, the relative performance of the data points is correct. This means that that both methods identify the same points as having better or worse performance, implying that the Markov model can be used for finding good tree parameters.

We note that one expected imperfection in the application of the Markov method is the use of bulk error and gate-count estimates. The method can be improved by using a more using the exact Clifford circuits and subcircuits to find gate counts and idle times. Moreover, other issues such as accurate error propagation are difficult to avoid without a direct simulation. The qualitative result should be sufficient to provide guidance for narrowing down the tree parameters before going into more accurate methods.

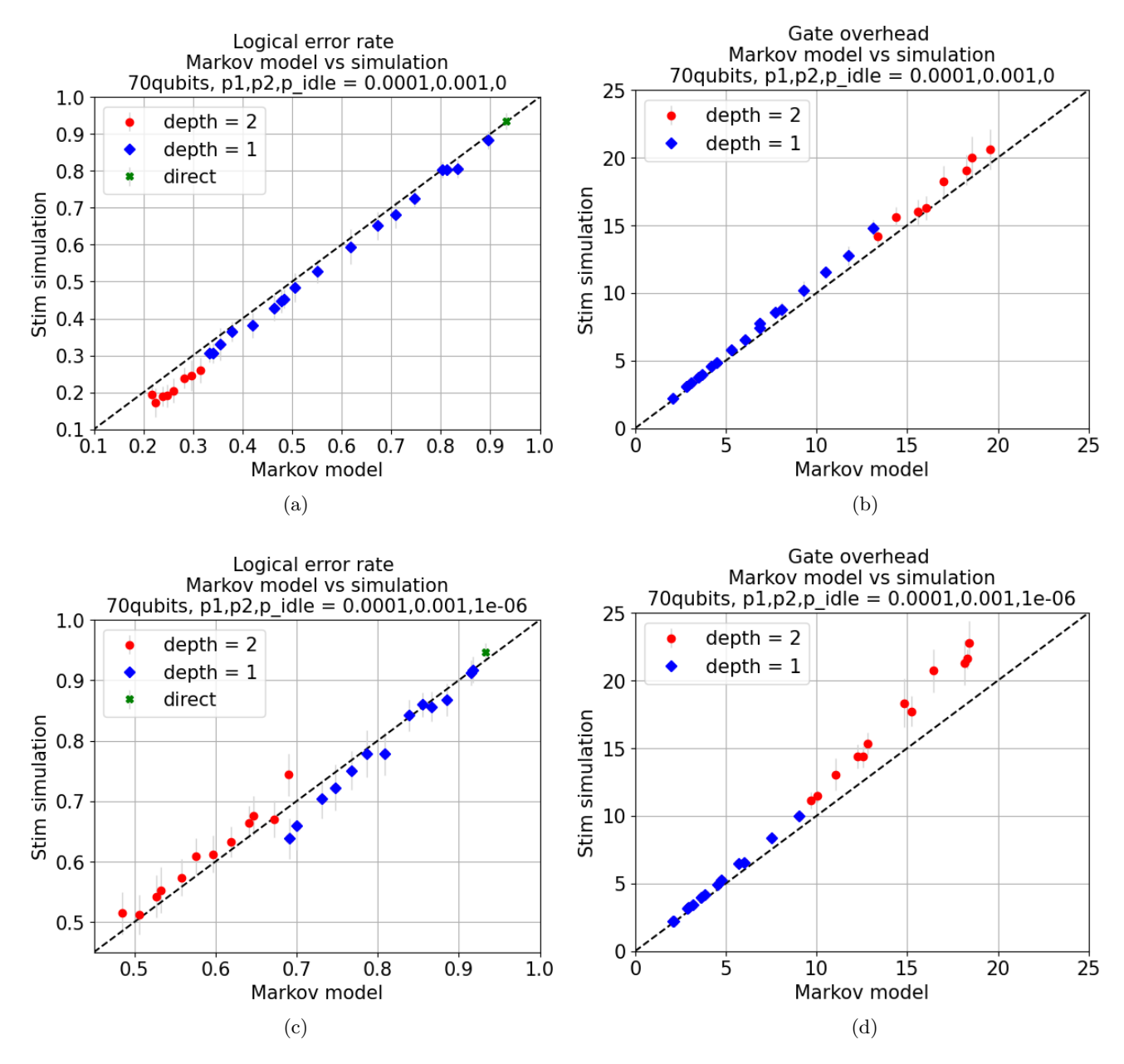


FIG. 6. Markov model compared with the Monte Carlo Stim based simulation.